VIROLOGY 213, 364–372 (1995)

Equine Arteritis Virus Subgenomic RNA Transcription: UV Inactivation and

JOHAN A. DEN BOON, WILLY J. M. SPAAN, and ERIC J. SNIJDER[1]

Department of Virology, Institute of Medical Microbiology, Faculty of Medicine, Leiden University, The Netherlands

Received June 9, 1995; accepted August 25, 1995

The expression of the genetic information of equine arteritis virus (EAV), an arterivirus, involves the synthesis of six subgenomic (sg) mRNAs. These are 5′ and 3′ coterminal since they are composed of a leader and a body sequence, which are identical to the 5′ and 3′ ends of the genome, respectively. Previously, it has been suggested that *cis*-splicing of a genome-length precursor RNA is involved in their synthesis. This was reevaluated in a comparative analysis of the sg RNA synthesis of EAV, the coronavirus mouse hepatitis virus (MHV), and the alphavirus Sindbis virus. UV transcription mapping showed that the majority of the EAV sg RNAs made at later stages of infection is not derived from a genome-length precursor. However, complete independence of sg RNA synthesis from that of genomic RNA was never observed during the course of infection. The possibility that this resulted from UV irradiation-induced effects on the synthesis of the viral replicase was investigated by inhibiting translation using cycloheximide. For EAV, ongoing protein synthesis was found to be more important for the synthesis of sg RNA than for that of genomic RNA. In general, MHV transcription was extremely sensitive to translation inhibition, whereas EAV genomic RNA synthesis became independent of *de novo* protein synthesis late in infection.

INTRODUCTION

Equine arteritis virus (EAV) is the type member of a recently reclassified group of enveloped positive-stranded RNA viruses, the arteriviruses (for a review: Plagemann and Moennig, 1992). Other arteriviruses are lactate dehydrogenase-elevating virus of mice (Godeny *et al.,* 1993), porcine reproductive and respiratory syndrome virus (Meulenberg *et al.,* 1993a), and simian hemorrhagic fever virus (Godeny *et al.,* 1995).

The sequence analysis of the EAV genome previously revealed that arteriviruses are evolutionarily related to corona- and toroviruses (den Boon *et al.,* 1991). Their common ancestry is illustrated by the presence of a number of homologous replicase domains and striking similarities in genome organization and expression. The EAV genome is a 12.7-kb RNA molecule which is structurally polycistronic (Fig. 1). From this RNA open reading frames (ORFs) 1a and 1b are translated into two large replicase polyproteins, 1a and 1ab, which are N-terminally identical but, due to ribosomal frameshifting, C-terminally different (den Boon *et al.,* 1991). The more distally located ORFs 2–7, which encode four structural proteins (de Vries *et al.,* 1992) and two proteins of unknown function, are expressed from a 3′ coterminal nested set of subgenomic (sg) RNAs (van Berlo *et al.,* 1982; de Vries *et al.,* 1990). As in the case of coronaviruses, the arterivirus sg RNAs are composed of sequences which are not contiguous in the genomic RNA (de Vries *et al.,* 1990). A common 5′ leader sequence of 206 nt, derived from the 5′ end of the genome, is fused to mRNA body sequences which are colinear with the genomic 3′ end. For EAV sg RNAs 6 and 7 the so-called leader–body junction site is a pentanucleotide sequence (5′ UCAAC 3′), present at the 3′ end of the leader sequence and at the 5′ end of the mRNA body (de Vries *et al.,* 1990).

Despite the structural similarities between arteri- and coronavirus sg RNAs, their modes of synthesis were reported to be different. Stern and Sefton (1982), Jacobs *et al.* (1981), and Yokomori *et al.* (1992) have used UV transcription mapping analyses to investigate coronavirus sg RNA synthesis. They showed that late in infection the UV sensitivity of the synthesis of the sg mRNAs is not equal to that of the genomic RNA. Instead, UV target sizes of subgenomic transcripts were concluded to be proportional to their physical size. In contrast, van Berlo *et al.* (1982) reported approximately identical UV target sizes for the genomic RNA and all sg RNAs of the arterivirus EAV. Although a slight deviation was observed for the smallest sg RNA, currently known as RNA 7, the data suggested a posttranscriptional processing mechanism that generates all sg RNAs from a genome-length precursor.

In view of the subsequently detected common ancestry of the arterivirus and coronavirus replicases, we considered it unlikely that their sg RNA transcription mecha-

[1] To whom correspondence and reprint requests should be addressed at: Department of Virology, Institute of Medical Microbiology, Leiden University, Postbus 320, 2300 AH Leiden, The Netherlands. Fax: 31-71263645. E-mail: SNIJDER@RULLF2.LeidenUniv.NL.

0042-6822/95 $12.00

nisms would be essentially different. Upon reexamination of the experimental details of the previous EAV UV transcription mapping analysis (van Berlo *et al.,* 1982), we found the applied UV doses to be remarkably low: a maximum dose of 300 erg · mm^{-2} was used. For comparison, the inactivation of the synthesis of sg RNA 2 of the coronavirus mouse hepatitis virus (MHV), which is only 3 kb smaller than the EAV genome, required UV doses of up to 3000 erg · mm^{-2} (Jacobs *et al.,* 1981). In view of these observations, we decided to repeat the experiments. A comparative analysis on the basis of new UV transcription mapping data for EAV, MHV, and the alphavirus Sindbis virus (SIN) is described in this paper. The latter was chosen as a reference because the genome sizes of EAV and SIN are similar and because the synthesis of the sg 26S RNA of SIN is known to be fully independent from that of the genome (Brzeski and Kennedy, 1978). In the context of these experiments, we have also studied the effect of translation inhibition by cycloheximide on the synthesis of viral RNA.

MATERIALS AND METHODS

Cells and viruses

Equine arteritis virus (Bucyrus strain) and SIN (HR strain) were grown in baby hamster kidney cells (BHK-21). Mouse hepatitis virus (MHV-A59) was propagated in Sac(−) or mouse L-cells. Experiments with EAV were carried out at 39.5°. Infections with SIN and MHV were performed at 37°.

Metabolic labeling and isolation of intracellular RNA

In order to measure RNA synthesis during specific time intervals in infection, the medium was replaced by medium containing 10 μg/ml of dactinomycin to block host RNA synthesis. After 30–60 min, cultures were incubated for 60–90 min in medium containing 100–500 μCi of [^{3}H]uridine and 10 μg/ml of dactinomycin. RNA lysates were prepared as described previously (Spaan *et al.,* 1981).

RNA electrophoresis

Denaturing RNA electrophoresis was carried out using 1–1.5% agarose gels containing 10 m*M* MOPS (morpholinepropanesulfonic acid) and 2.2 *M* formaldehyde. For analysis of ^{3}H-labeled RNA samples, agarose gels were fixed in methanol, impregnated with 3% PPO (2,5-diphenyloxazole) in methanol, rinsed with water, and dried at 60°. After fluorography, incorporation of label into individual RNA species was quantified by excision of bands from dried gels and scintillation counting.

UV transcription mapping

For UV transcription mapping of EAV, BHK-21 cells were infected with an m.o.i. of 50. At $6\frac{1}{2}$ hr p.i., the medium was removed, and cells were UV-irradiated for various intervals with a dose rate of 40 erg · s^{-1} · mm^{-2} (the total dose was between 0 and 3600 erg · mm^{-2}). Following irradiation, RNA was metabolically labeled for 60 min. For MHV, UV transcription mapping experiments were repeated at 6 hr p.i. under the conditions described by Jacobs *et al.* (1981). UV transcription mapping of SIN-infected cells (m.o.i. 100) was carried out at 4 hr p.i., applying the same irradiation doses used for EAV. UV target sizes (*T*) were calculated according to the equation: $\ln(N_t/N_0) = -K \times T \times t$. N_t is the rate

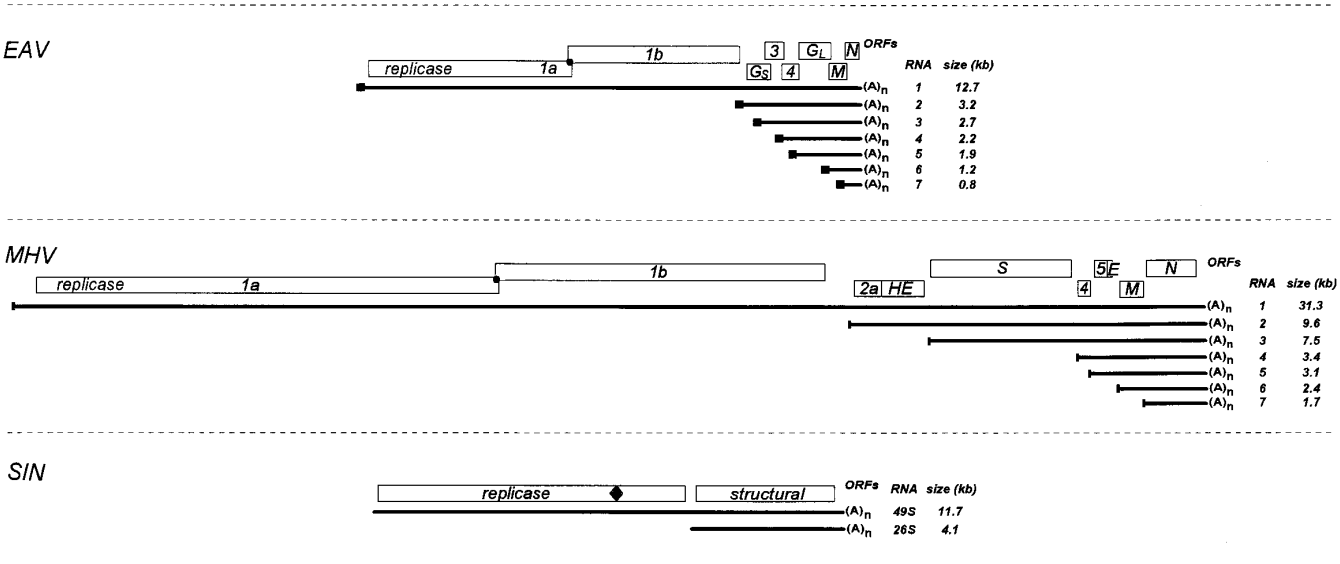

FIG. 1. The EAV, MHV, and SIN genome organizations: the 3′ coterminal nested sets of genomic and subgenomic RNAs, and the positions of the ORFs. The boxes at the 5′ ends of the EAV and MHV RNAs represent the common leader sequence. The positions where ribosomal frameshifting (EAV/MHV) or readthrough (SIN) occurs during translation of the replicase gene are indicated.

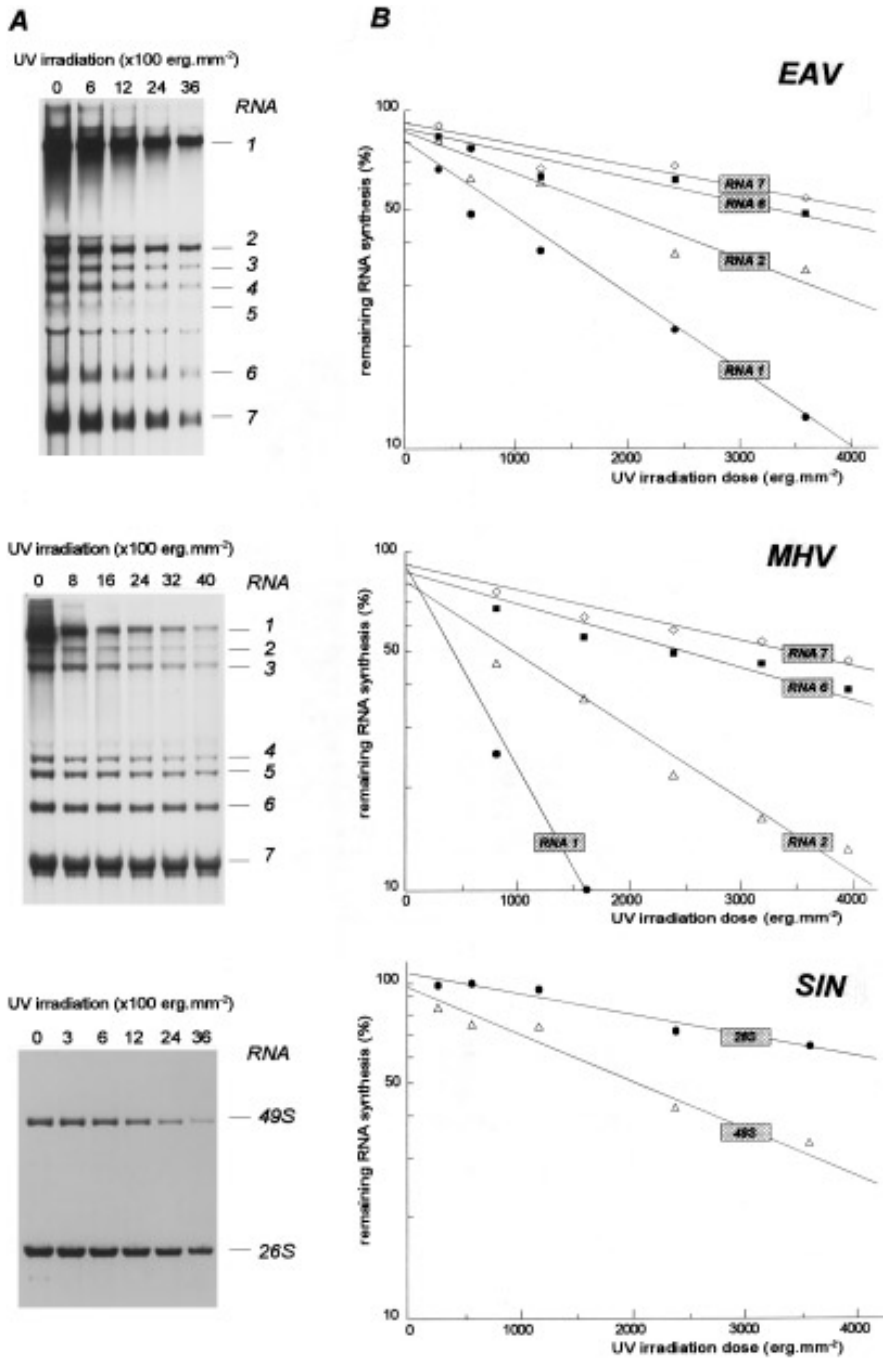

FIG. 2. UV transcription mapping analysis of EAV ($6\frac{1}{2}$ hr p.i.), MHV (6 hr p.i.), and SIN (4 hr p.i.) RNA synthesis. (A) Representative fluorographs. Infected cells were UV-irradiated with increasing doses and subsequently metabolically labeled using [^{3}H]uridine. Denaturing agarose gel electrophoresis was performed to resolve the individual RNAs. (B) RNAs 1, 2, 6, and 7 (EAV and MHV) or 49S and 26S RNAs (SIN) were excised from gel for quantification by scintillation counting. The remaining RNA synthesis relative to the nonirradiated control is plotted against irradiation doses. Curves were fitted using linear regression analysis.

of RNA synthesis after t sec of irradiation, N_0 that of the unirradiated control, and K is a constant (Sauerbier and Hercules, 1978). Curves were fitted using linear regression analysis.

In a separate experiment, the effect of UV irradiation at different time points in infection was investigated. EAV-infected BHK-21 cells were UV-irradiated with a single dose of 2400 erg · mm^{-2} at 4, 5, or 6 hr p.i., and metabolically labeled RNA was subsequently analyzed as described.

Inhibition of protein synthesis

Protein synthesis was inhibited by replacing the medium with medium containing 100 μg/ml of cyclohexi-

mide. The same concentration of the drug was present during metabolic labeling of the intracellular RNA.

RESULTS

EAV sg RNAs are not derived from genome-length precursor RNA

UV irradiation induces the formation of uracil dimers, which, at the position of the lesion, inactivate the RNA molecule as a transcription template (Sauerbier and Hercules, 1978). It is assumed (i) that one hit is sufficient to inactivate RNA transcription from a given transcription unit, (ii) that repair is insignificant or absent, and (iii) that the number of hits is proportional to the irradiation dose and the size of the transcription unit. Thus, the UV transcription mapping technique can be used to determine whether multiple RNA transcripts, such as the sg RNAs found in EAV-infected cells, are derived from the same precursor molecule. If so, the sensitivity of their synthesis to UV irradiation (UV target size) will for all sg RNAs be identical to the target size of that precursor. Alternatively, when the transcription of sg RNAs is fully independent from that of the genome, a UV target size which is proportional to its physical size should be measured for each sg RNA.

EAV-infected BHK-21 cells were UV-irradiated at $6\frac{1}{2}$ hr p.i., when RNA synthesis approaches its maximum (van Berlo *et al.,* 1982, and data not shown). Subsequently, viral RNA synthesis was monitored by [^{3}H]uridine incorporation. In parallel, ^{3}H-labeled RNA was isolated from MHV-infected cells which were UV-irradiated at 6 hr p.i. To determine the UV inactivation kinetics for individual RNA species, ^{3}H-labeled RNAs were separated in denaturing agarose gels. Representative fluorographs for both viruses are shown in Fig. 2A. For both EAV and MHV, we restricted our analysis to the genomic RNA and three sg RNAs (2, 6, and 7). Bands were cut from four agarose gels, derived from two independent experiments. In Fig. 2B the average percentages of remaining RNA synthesis have been plotted against the UV dose. These graphs clearly show that for both viruses the sg RNA synthesis is not directly dependent on the synthesis of a genome-length precursor RNA. On the other hand, the UV target sizes of the RNAs, which are reflected by the slopes of the curves, are not proportional to their physical sizes either (Table 1). Compared to the genomic RNA, the synthesis of sg RNAs of both EAV and MHV is more sensitive to UV irradiation than would be expected on the basis of their lengths.

Sindbis virus UV transcription mapping

To investigate whether the discrepancy between relative physical sizes and UV target sizes of genomic and sg RNAs is typical of arteri- and coronavirus transcription, a UV transcription mapping analysis was carried out for the well-characterized alphavirus SIN, using the same irradiation doses and the same BHK-21 cells used for the EAV analysis. The length of the 49S SIN genomic RNA (11.7 kb) is comparable to that of EAV (12.7 kb) (Fig. 1). The replication of SIN involves the synthesis of a single 4.1-kb sg RNA (26S) from a well-defined internal promoter on the genome-sized minus-strand template RNA (Ou *et al.,* 1982; Levis *et al.,* 1990). As shown in Fig. 2 and Table 1, the relative physical and UV target sizes of the genomic and sg SIN transcripts were in good agreement, as was previously shown by Brzeski and Kennedy (1978). In addition to this difference with the corona- and arterivirus systems, SIN transcription in general was less sensitive to UV irradiation than EAV and MHV transcription.

TABLE 1

Comparison of the (Relative) Physical and Relative UV Target Sizes for EAV, MHV, and SIN RNAs

	RNA[a]	Physical size (kb)	Relative physical size	Relative UV target size
EAV	1	12.7	100	100
	2	3.2	25.1	54.0
	6	1.0	7.8	32.4
	7	0.7	5.5	27.0
MHV	1	31.3	100	100
	2	9.6	30.6	28.4
	6	2.4	7.7	14.8
	7	1.7	5.4	12.3
SIN	49S	11.7	100	100
	26S	4.1	35.0	38.5

[a] RNA sizes were obtained from den Boon *et al.* (1991), references cited in Spaan *et al.* (1988), and Strauss *et al.* (1984).

UV irradiation has differential effects early and late in EAV infection

Yokomori *et al.* (1992) showed that during the early stages of MHV infection the UV target sizes of sg RNAs approach that of the genomic RNA. This observation prompted us to compare the UV target sizes of the EAV transcripts at three different time points in infection. In Fig. 3 the reduction in the synthesis of RNAs 1, 2, 6, and 7 is compared after UV irradiation with a single dose (2400 erg · mm^{-2}) at 4, 5, or 6 hr p.i. and subsequent metabolic labeling for 1 hr. Quantitative analysis on the basis of two experiments showed that, similar to the situation in coronavirus-infected cells, UV sensitivities during early and late transcription were different. Upon irradiation at 4 or 5 hr p.i. the relative decrease in the synthesis of the genomic and sg RNAs was similar, whereas after irradiation at 6 hr p.i. sg RNA synthesis was less affected than that of RNA 1 (Fig. 3B).

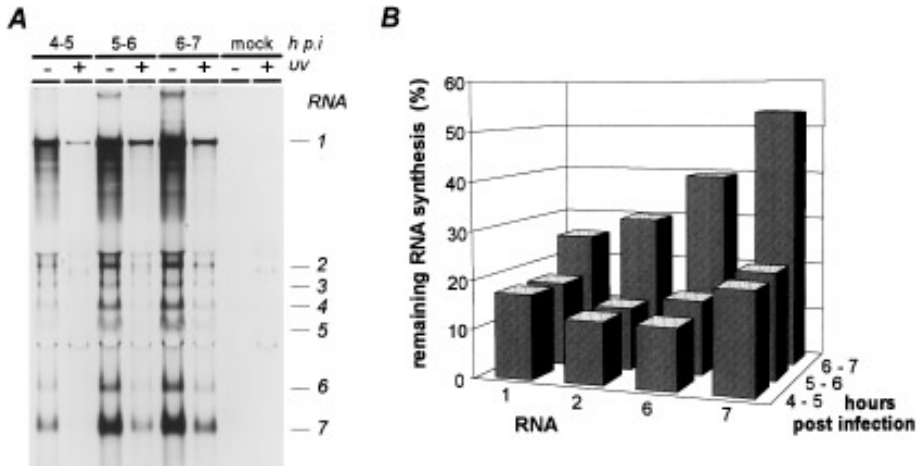

FIG. 3. UV transcription inactivation, early vs late, in EAV infection. At three time points in infection, EAV or mock-infected cells were UV-irradiated using a single dose of 2400 erg · mm^{-2}, and intracellular RNA was subsequently metabolically labeled for 1 hr. (A) Representative fluorograph of [^{3}H]uridine-labeled RNA resolved by denaturing agarose gel electrophoresis. (B) Quantitative analysis of the reduction in the synthesis of RNAs 1, 2, 6, and 7 relative to the nonirradiated control. Mean values were calculated on the basis of two separate experiments, after determination of the [^{3}H]uridine incorporation in individual RNAs excised from four dried gels.

Requirement of protein synthesis for RNA transcription

The UV transcription mapping data showed that the EAV sg RNAs were not produced by processing of a genome-length precursor RNA. However, unlike the case of the SIN sg RNA, their UV target sizes were larger than expected on the basis of their physical sizes, even when sg RNA synthesis had reached its maximum. The genomic RNA encodes the viral replicase, which is involved in both genomic and sg RNA synthesis. Thus, its inactivation as a transcription unit by UV irradiation could have an important side effect: reduction of the amount of mRNA for replicase synthesis. Depending on the requirement of *de novo* replicase synthesis for sg RNA transcription, it was feasible that the UV inactivation of genomic RNA synthesis indirectly influenced the production of sg RNAs, which would therefore never become completely independent.

We investigated to what extent EAV RNA synthesis depended on continuous protein synthesis and whether the UV transcription mapping results could be explained by a combined effect on transcription and replicase translation. Protein synthesis was inhibited by the addition of cycloheximide to EAV-infected BHK-21 cells at different time points after infection. One hour later, the effect of translation inhibition on RNA synthesis was measured by metabolic labeling. RNAs were isolated and analyzed by denaturing gel electrophoresis (Fig. 4). For comparison, similar analyses with MHV and SIN were carried out.

On the basis of these experiments a number of conclusions could be drawn. First, ongoing protein synthesis was most important during the early phase of infection. Second, compared to genomic RNA synthesis, EAV sg RNA synthesis was more dependent on protein synthesis. This was irrespective of the stage of infection. As previously reported by Sawicki and Sawicki (1986), this differential dependence was not observed for MHV. Third, the overall MHV transcription was significantly more dependent on *de novo* protein synthesis than that of EAV and SIN. Even during the late phase of the MHV infection cycle, when all infected cells were fused into one large syncytium, both genomic and sg RNA synthesis were severely impaired by the addition of cycloheximide. In contrast, EAV genomic RNA synthesis was nearly translation-independent late in infection. In the case of SIN, the transcription of 49S genomic RNA was less affected than that of 26S sg RNA during the earlier stages of infection, but the synthesis of both became largely translation-independent as infection progressed. Late in infection, 26S RNA transcription was even less affected by translation inhibition than 49S transcription.

DISCUSSION

The EAV UV inactivation experiments described in this paper show that at the peak of sg RNA synthesis conventional *cis*-splicing, if at all, is not a major mechanism in the production of the EAV sg mRNAs. However, in a fully independent transcription system the slopes of the curves in Fig. 2B, which reflect the UV target sizes, should be directly proportional to the physical sizes of the transcription units. In that case, the transcription of e.g., the EAV genome (12.7 kb) would be expected to be 18 times more sensitive to UV irradiation than the synthesis of the smallest sg RNA, RNA 7 (0.7 kb). It is clear that the relative RNA sizes and relative UV sensitivities (Table 1) do not support the conclusion that the transcription of the EAV genomic and sg RNAs are fully independent.

A similar analysis of our MHV data (Table 1) also revealed that the transcription of the sg RNAs of coronavi-

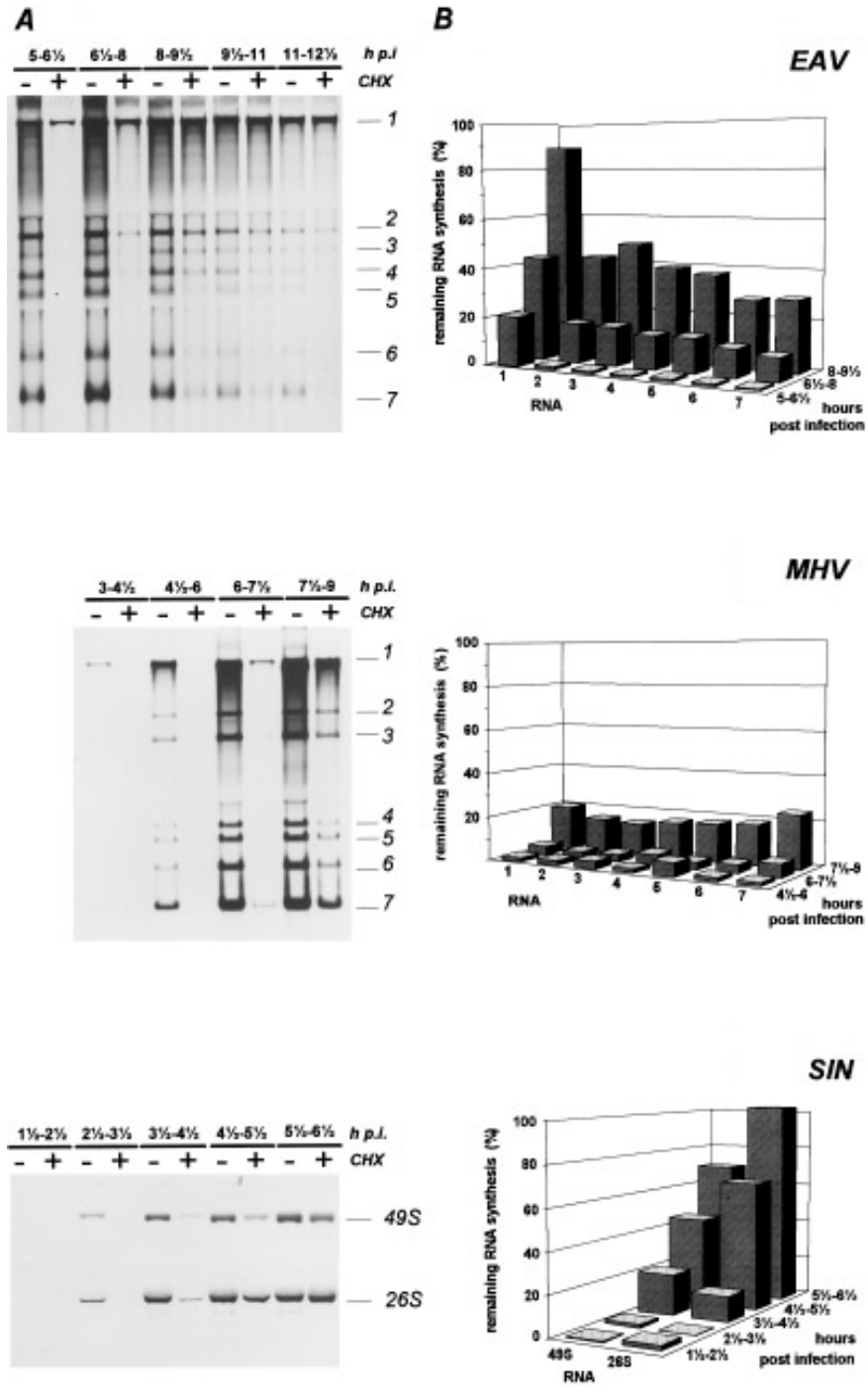

FIG. 4. The effect of translation inhibition on EAV, MHV, and SIN RNA transcription. (A) Fluorographs showing the effects of cycloheximide addition (100 μg/ml) as compared to the untreated control at the indicated time intervals. RNA synthesis was monitored by metabolic labeling using [^{3}H]uridine, either in the absence or in the presence of cycloheximide, and RNAs were analyzed by denaturing agarose gel electrophoresis. (B) Individual RNAs were excised from gel and quantified by scintillation counting. The calculated reduction in genomic and sg RNA synthesis in the presence of cycloheximide is displayed relative to the untreated control.

ruses is not fully independent from that of genomic RNA. As for EAV, there are clear differences in UV sensitivity between larger and smaller RNAs, but the quantitative MHV analysis shows differences between relative physical sizes and relative UV sensitivities. Our results are in general agreement with those which have previously been published by Jacobs *et al.* (1981) and Yokomori *et al.* (1992). Both groups reported differences between the UV target sizes of the various MHV RNAs which are in the same range as our observations. For example, the UV target size of MHV RNA 7 calculated by Jacobs *et al.* (1981) is only about eight times smaller than that of geno-

mic RNA, whereas the physical size ratio is about 1:18. Due to the fact that at that time the length of the MHV genome was assumed to be only 16 kb, instead of the currently known 31 kb, Jacobs *et al.* (1981) concluded that their data supported fully independent transcription of MHV genomic and sg RNAs. Yokomori *et al.* (1992), who recently repeated the MHV UV transcription mapping experiments, did not describe a detailed quantitative analysis of the data they obtained late in infection, but concluded that UV sensitivities roughly paralleled mRNA sizes. However, a calculation using the graphs published by Yokomori *et al.* (1992) revealed only a sevenfold difference between the genomic RNA and RNA 7. Similar observations were made when we reevaluated the data obtained with another coronavirus, infectious bronchitis virus (Stern and Sefton, 1982).

Our UV transcription mapping in SIN-infected cells resulted in an almost perfect correlation between physical RNA sizes and UV target sizes (Fig. 2; Table 1). These results demonstrate that the experimental approach was appropriate and that our observations for EAV cannot be explained by technical imperfections. Apparently, the intrinsic properties of coronavirus-like RNA transcription are different from those of alphaviruses.

Although *cis*-splicing events cannot be ruled out as an early-stage mechanism to produce sg RNAs, another transcription mechanism must be operating in EAV-infected cells and is most likely similar to that of coronaviruses. The so-called leader-primed transcription model has been proposed to explain the synthesis of coronavirus sg RNAs (Baric *et al.,* 1983; Spaan *et al.,* 1983) and a substantial amount of data in its favor has been reported (for a review: Spaan *et al.,* 1988; Lai, 1990). According to this model, sg RNAs are synthesized either by an intrinsic ability of the viral leader/polymerase complex to dissociate from its template and subsequently resume synthesis at a more distal position or by priming by free leader transcripts at subgenomic promoter sequences (the complements of the so-called intergenic sequences on the positive strand). The conserved leader–body junction sequences in EAV sg RNAs (de Vries *et al.,* 1990; den Boon *et al.,* manuscript in preparation) possibly represent such complementary promoter sequences. Similar sequence elements have been described for other arteriviruses (Godeny *et al.,* 1993; Conzelmann *et al.,* 1993; Chen *et al.,* 1993; Meulenberg *et al.,* 1993b; Zeng *et al.,* 1995). A single genome-length minus-strand RNA could be the template used for the synthesis of genomic as well as sg mRNAs. Nevertheless, anti-leader-containing subgenomic minus strands in coronavirus-infected cells have been demonstrated (Hofmann *et al.,* 1990; Sethna *et al.,* 1989, 1991). Their presence in double-stranded replicative intermediates suggests that these might function in mRNA transcription (Sawicki and Sawicki, 1990). On the basis of these and other observations several coronavirus transcription

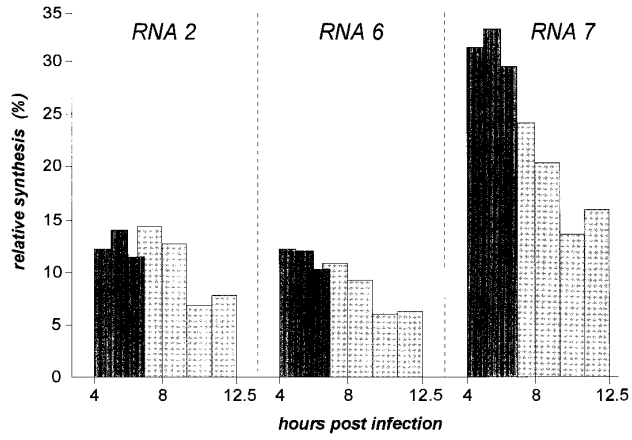

FIG. 5. The synthesis of sg RNAs 2, 6, and 7, relative to that of the genomic RNA, during different time intervals throughout infection. Data are derived from the untreated infected cells in the experiments described in Figs. 3 (dark shading) and 4 (light shading).

models have been put forward, which are not necessarily mutually exclusive (Jeong and Makino, 1994; Sawicki and Sawicki, 1990; van der Most *et al.,* 1994). Leader-primed transcription could, for example, generate a first generation of sg mRNAs, which could subsequently function as templates for sg minus-strand production. These could in turn be used to transcribe a second generation of positive-strand sg mRNAs. The recent analysis of the transcriptional activity of a number of MHV ts-mutants indicates that sg minus strands are likely to be used as transcription templates late in infection (Schaad and Baric, 1994). Like the UV transcription mapping results described for MHV (Yokomori *et al.,* 1992), our data on EAV indicate that different mechanisms of sg RNA transcription might be operating simultaneously. The differences in UV sensitivity of sg RNA synthesis early and late in infection (Fig. 3) can be interpreted to reflect the levels at which each of these mechanisms participate in transcription, at a given stage in infection.

We have considered the possibility that replicase synthesis was affected by UV irradiation and that genomic and sg RNA synthesis were inhibited as a result. Differential effects of translation inhibition early vs late in infection (Fig. 4) may be based on the properties as well as the absolute amount of the replicase. Our results and previously published data from Sawicki and Sawicki (1986) on MHV RNA transcription indicated that ongoing protein synthesis is an absolute requirement during the early stages of infection and that both MHV genomic and sg RNA synthesis at later stages were still significantly reduced when translation was blocked. In contrast, the EAV data indicated that the synthesis of sg RNAs was more impaired by inhibition of translation than was the case for the production of genomic RNA. In addition, the data presented in Figs. 3 and 4 revealed that sg RNA synthesis is down-regulated relative to the synthesis of genomic RNA late in infection (Fig. 5).

Whether our findings are indicative of a functional polymerase switch, from synthesizing sg RNA to producing genomic RNA, remains to be investigated. Similar to the regulatory function of nonstructural polyprotein processing in alphavirus replication (for a review: Strauss and Strauss, 1994), proteolytic processing may influence the transcriptional specificity of the replicase in arteriviruses. The current model for SIN transcription includes a temporal switch from negative to plus-strand RNA synthesis, regulated by posttranslational replicase processing. In agreement with our results, this conversion of replicase complexes indeed makes positive-strand RNA synthesis independent of *de novo* protein synthesis, since it is a relatively late function of the replicase complex.

Our current analysis of the processing of the EAV replicase polyprotein has already revealed rapid and slow proteolytic cleavages (Snijder *et al.,* 1994). A slow conformational change of the replicase complex in favor of genome replication may provide an explanation for the discrepancy between physical sizes and UV target sizes of sg RNAs compared to genome transcription. EAV sg RNA synthesis could be more dependent on *de novo* replicase synthesis, which in turn depends on the level of replicase mRNA (i.e., genomic RNA). UV-induced reduction of genome synthesis would then lead to reduced replicase translation, which would cause a decrease in sg RNA synthesis relative to genomic RNA synthesis. Together with the direct UV sensitivity of the sg RNA transcription units, the more indirect effect of translation dependence would be reflected in observed UV target sizes and could thus, at least partially, explain the discrepancy found between physical and UV target sizes. An alternative explanation for the observed difference in sensitivity to translation inhibition between genomic and sg RNA synthesis could be a demand for one or more relatively instable host protein factors involved in sg RNA transcription, the synthesis of which might be affected by UV irradiation.

In conclusion, our hypothesis that, in view of their ancestral relationship, arterivirus sg RNA transcription should resemble that of coronaviruses is now supported by experimental data. In spite of basic similarities, there appear to be specific regulatory differences as well. To investigate these in more detail, we are currently focusing our attention on the analysis of EAV minus-strand RNA and replicative intermediates.

ACKNOWLEDGMENTS

We thank Fred Wassenaar, Leonie van Dinten, and Dorothea and Stanley Sawicki for stimulating discussions and helpful comments on the manuscript.

REFERENCES

Baric, R. S., Stohlman, S. A., and Lai, M. M. C. (1983). Characterization of replicative intermediate RNA of mouse hepatitis virus: Presence of leader RNA sequences on nascent chains. *J. Virol.* 48, 633–640.

Brzeski, H., and Kennedy, S. I. T. (1978). Synthesis of alphavirus-specified RNA. *J. Virol.* 25, 630–640.

Chen, Z., Kuo, L., Rowland, R. R. R., Even, C., Faaberg, K. S., and Plagemann, P. G. W. (1993). Sequence of 3′ end of genome and of 5′ end of ORF 1a of lactate dehydrogenase-elevating virus (LDV) and common junction motifs between 5′ leader and bodies of seven subgenomic mRNAs. *J. Gen. Virol.* 74, 643–660.

Conzelmann, K. K., Visser, N., Woensel, P. V., and Thiel, H. J. (1993). Molecular characterization of porcine reproductive and respiratory syndrome virus, a member of the arterivirus group. *Virology* 193, 329–339.

Den Boon, J. A., Snijder, E. J., Chirnside, E. D., De Vries, A. A. F., Horzinek, M. C., and Spaan, W. J. M. (1991). Equine arteritis virus is not a togavirus but belongs to the coronaviruslike superfamily. *J. Virol.* 65, 2910–2920.

De Vries, A. A. F., Chirnside, E. D., Bredenbeek, P. J., Gravestein, L. A., Horzinek, M. C., and Spaan, W. J. M. (1990). All subgenomic mRNAs of equine arteritis virus contain a common leader sequence. *Nucleic Acids Res.* 18, 3241–3247.

De Vries, A. A. F., Chirnside, E. D., Horzinek, M. C., and Rottier, P. J. (1992). Structural proteins of equine arteritis virus. *J. Virol.* 66, 6294–6303.

Godeny, E. K., Chen, L., Kumar, S. N., Methven, S. L., Koonin, E. V., and Brinton, M. A. (1993). Complete genomic sequence and phylogenetic analysis of the lactate dehydrogenase-elevating virus. *Virology* 194, 585–596.

Godeny, E. K., Zeng, L., Smith, S. L., and Brinton, M. A. (1995). Molecular characterization of the 3′ terminus of the simian hemorrhagic fever virus genome. *J. Virol.* 69, 2679–2683.

Hofmann, M. A., Sethna, P. B., and Brian, D. A. (1990). Bovine coronavirus mRNA replication continues throughout persistent infection in cell culture. *J. Virol.* 64, 4108–4114.

Jacobs, L., Spaan, W. J. M., Horzinek, M. C., and Van der Zeijst, B. A. M. (1981). Synthesis of subgenomic mRNA's of mouse hepatitis virus is initiated independently: Evidence from UV transcription mapping. *J. Virol.* 39, 401–406.

Jeong, Y. S., and Makino, S. (1994). Mechanism of coronavirus transcription: Duration of primary transcription initiation activity and effects of subgenomic RNA transcription on RNA replication. *J. Virol.* 66, 3339–3346.

Lai, M. M. C. (1990). Coronavirus—Organization, replication and expression of genome. *Annu. Rev. Microbiol.* 44, 303–333.

Levis, R., Schlesinger, S., and Huang, H. V. (1990). Promoter for Sindbis virus RNA-dependent subgenomic RNA transcription. *J. Virol.* 64, 1726–1733.

Meulenberg, J. J. M., Hulst, M. M., De Meijer, E. J., Moonen, P. L. J. M., Den Besten, A., De Kluyver, E. P., Wensvoort, G., and Moormann, R. J. M. (1993a). Lelystad virus, the causative agent of porcine epidemic abortion and respiratory syndrome (PEARS), is related to LDV and EAV. *Virology* 192, 62–72.

Meulenberg, J. J. M., De Meijer, E. J., and Moormann, R. J. M. (1993b). Subgenomic RNAs of Lelystad virus contain a conserved leader-body junction sequence. *J. Gen. Virol.* 74, 1697–1701.

Ou, J.-H., Rice, C. M., Dalgarno, L., Strauss, E. G., and Strauss, J. H. (1982). Sequence studies of several alphavirus genomic RNAs in the region containing the start of the subgenomic RNA. *Proc. Natl. Acad. Sci. USA* 79, 5235–5239.

Plagemann, P. G. W., and Moennig, V. (1992). Lactate dehydrogenase-elevating virus, equine arteritis virus and simian haemorrhagic fever virus, a new group of positive strand RNA viruses. *Adv. Virus Res.* 41, 99–192.

Sauerbier, W., and Hercules, K. (1978). Gene and transcription unit mapping by radiation effects. *Annu. Rev. Genet.* 12, 329–363.

Sawicki, S. G., and Sawicki, D. L. (1986). Coronavirus minus-strand synthesis and effect of cycloheximide on coronavirus RNA synthesis. *J. Virol.* 57, 328–334.

Sawicki, S. G., and Sawicki, D. L. (1990). Coronavirus transcription:

Subgenomic mouse hepatitis virus replicative intermediates function in RNA synthesis. *J. Virol.* 64, 1050–1056.

Schaad, M. C., and Baric, R. S. (1994). Genetics of mouse hepatitis virus transcription: Evidence that subgenomic negative strands are functional templates. *J. Virol.* 68, 8169–8179.

Sethna, P. B., Hofmann, N. A., and Brian, D. A. (1991). Minus-strand copies of replicating coronavirus mRNAs contain anti-leaders. *J. Virol.* 65, 320–325.

Sethna, P. B., Hung, S. L., and Brian, D. A. (1989). Coronavirus subgenomic minus-strand RNAs and the potential for mRNA replicons. *Proc. Natl. Acad. Sci. USA* 86, 5626–5630.

Snijder, E. J., Wassenaar, A. L. M., and Spaan, W. J. M. (1994). Proteolytic processing of the replicase ORF1a protein of equine arteritis virus. *J. Virol.* 68, 5755–5764.

Spaan, W. J. M., Rottier, P. J. M., Horzinek, M. C., and Van der Zeijst, B. A. M. (1981). Isolation and identification of virus-specific mRNAs in cells infected with mouse hepatitis virus (MHV-A59). *Virology* 108, 424–434.

Spaan, W. J. M., Delius, H., Skinner, M., Armstrong, J., Rottier, P. J. M., Smeekens, S., van der Zeijst, B. A. M., and Siddell, S. G. (1983). Coronavirus mRNA synthesis involves fusion of non-contiguous sequences. *EMBO J.* 2, 1839–1844.

Spaan, W. J. M., Cavanagh, D., and Horzinek, M. C. (1988). Coronaviruses: Structure and genome expression. *J. Gen. Virol.* 69, 2939–2952.

Stern, D. F., and Sefton, B. M. (1982). Synthesis of coronavirus mRNAs: Kinetics of inactivation of infectious bronchitis virus RNA synthesis by UV light. *J. Virol.* 42, 755–759.

Strauss, E. G., Rice, C. M., and Strauss, J. H. (1984). Complete nucleotide sequence of the genomic RNA of Sindbis virus. *Virology* 133, 92–110.

Strauss, J. H., and Strauss, E. G. (1994). The alphaviruses: Gene expression, replication, and evolution. *Microbiol. Rev.* 58, 491–562.

Van Berlo, M. F., Horzinek, M. C., and Van der Zeijst, B. A. M. (1982). Equine arteritis virus-infected cells contain six polyadenylated virus-specific RNAs. *Virology* 118, 345–352.

Van der Most, R. G., de Groot, R. J., and Spaan, W. J. M. (1994). Subgenomic RNA synthesis directed by a synthetic defective interfering RNA of mouse hepatitis virus: A study of coronavirus transcription initiation. *J. Virol.* 68, 3656–3666.

Yokomori, K., Banner, L. R., and Lai, M. C. (1992). Coronavirus mRNA transcription: UV light transcriptional mapping studies suggest an early requirement for a genomic-length template. *J. Virol.* 66, 4671–4678.

Zeng, L., Godeny, E. K., Methven, S. L., and Brinton, M. A. (1995). Analysis of simian hemorrhagic fever virus (SHFV) subgenomic RNAs, junction sequences, and 5′ leader. *Virology* 207, 543–548.